Sensors and Materials, Vol. 8, No. 5 (1996) 251– 269
MYU Tokyo

S & M 0244

Modeling Electrostatically Deflectable Microstructures and Air Damping Effects

H. M. Reuther, M. Weinmann[1]*, M. Fischer, W. von Münch and F. Aßmus[1]

Stuttgart University, Institute of Semiconductor Engineering
Breitscheidstraße 2, 70174 Stuttgart, FRG
[1]Stuttgart University, Institute of Time Measurement and Precision Engineering
Breitscheidstraße 2b, 70174 Stuttgart, FRG

(Received February 28, 1994; accepted August 1, 1995)

Key words: Coupling of heterogeneous simulation tools, modeling of microstructures, air damping effects, quartz resonator, electrostatically deflectable polysilicon microstructures, modeling of electrostatic fields, modeling of hydrodynamic fields

Simulating the behavior of micromachined structures is essential to understand or predict their properties. Since the different effects influencing the behavior of the microstructures must be simulated with special simulation tools, these tools are coupled. As an example, the simulation of the deflection of a surface-micromachined polysilicon cantilever driven by electrostatic forces is presented in this paper. The calculated overall deflection of the cantilever is compared with experimental results. The contour of the cantilever during deflection due to the applied electrostatic field can be precisely predicted by the simulation. On the other hand, the vibration of a piezoelectrically driven quartz resonator oscillating in air is simulated. Exact knowledge of the velocity field of the surrounding air is important in order to improve the performance of such a quartz resonator, if it is used as a noncontact profile sensor. In this work, the FEM program FIDAP is used for hydrodynamic simulations and the FEM program ANSYS is applied for electrostatic, piezoelectric and mechanical simulations. Problems with simple geometry are simulated and the results are compared with the analytical solutions so the calculations can be verified. An alternative to the comparison with analytically solvable models is comparing the simulated behavior of the microstructures with experimental results. The described method of modeling microsystems and their dependence on external fields suggests a possible way to understand the properties of microsensors in order to improve their selectivity and sensitivity by coupling simulation tools and using them instead of experiments.

*Present address: Festo KG, Ruiter Straße 82, D-73734 Esslingen

1. Introduction

In order to improve the shape of microactuators or the sensitivity and selectivity of microsensors, the effects governing the behavior of the microstructures must be understood. Since the size of these microstructures generally does not allow a close-up look at the interactions leading to this behavior, other methods are necessary to investigate the microstructures. Numerical simulation of the behavior of the microstructures is a possibility. In contrast to Korvink *et al.*[1] where a special toolbox for the simulation of integrated micro-electromechanical systems is described, the approach presented in this paper uses finite-element (FE) simulation tools that are commercially available. It is not necessary to examine the behavior of the applied simulation tool since this is well known. The overall accuracy of the coupled simulation depends directly on the accuracy of the single simulation tool which is also well known. Therefore it is not the aim of this paper to deal with the numerical behavior of the simulation tools used. Those tools are specialized to simulate one specific effect. This requires that several tools are to be coupled. Hence, the simulation tools can be used instead of experiments. Verification of the simulation is possible by comparison with experimental results. However, for the development of the coupled simulation routines, another method of verification must be utilized. The calculation of analytically solvable models with a fairly simple geometry offers a comparison with the results of the numerical simulation. Two examples for such simulations are presented: the deflection of a cantilever under the influence of an electrostatic field and the air damping effects on oscillating quartz sensors.

In this work, the behavior of an electrostatically driven surface-micromachined polysilicon cantilever is simulated. A cantilever as shown in Fig. 1 has a thickness of 1 μm, and its width and length are 21.5 μm and 114 μm, respectively. The cantilever is 2 μm above the silicon substrate. The simulation of this cantilever follows the suggestions made

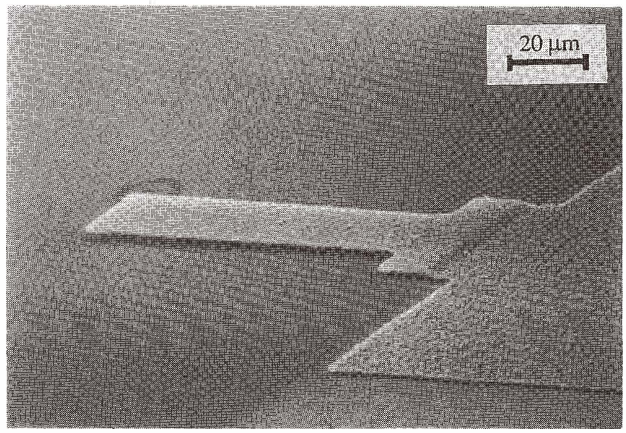

Fig. 1. SEM micrograph of a surface-micromachined polysilicon cantilever.

by Sheerer *et al.*[2] The applied routines are verified by comparing the analytical solution of a conducting sphere over an infinite surface with the results of the simulation of this problem. Using this model, the parameters of the mesh used for the FEM model can be optimized. The coupling between the electrostatic and the elastomechanic simulation and the movement of the mesh used for the electrostatic simulations constitute a main part of the work. Experimental results obtained for the deflection of a cantilever like the one shown in Fig. 1 under the influence of a voltage applied between the cantilever and the substrate are compared with the deflection results from the simulation.

On the other hand, the physical effects occurring on oscillating structures are of special interest. The properties of extensional-mode and tuning-fork quartz resonators, presented as noncontact profile sensors by Güthner[3] and Weinmann and co-workers,[4,5] are examined more closely in this work. The extensional-mode quartz resonator oscillates with a frequency of approximately 1 MHz, its tip has a cross-sectional area of about 80 μm $\times$ 120 μm and it is about 1.3 mm long. An SEM micrograph of this resonator is shown in Fig. 2.

The simulations of the hydrodynamic field are performed with the FEM program FIDAP, while the simulation of the piezoelectric movement of the resonator is carried out with the FEM program ANSYS. The coupling of these two simulations is described in this work.

The time-dependent hydrodynamic simulations are verified by comparing the analytical solution of a sphere oscillating in air with the results obtained from the simulation of this problem. Before introducing these simulations, some techniques used for the simulations are presented.

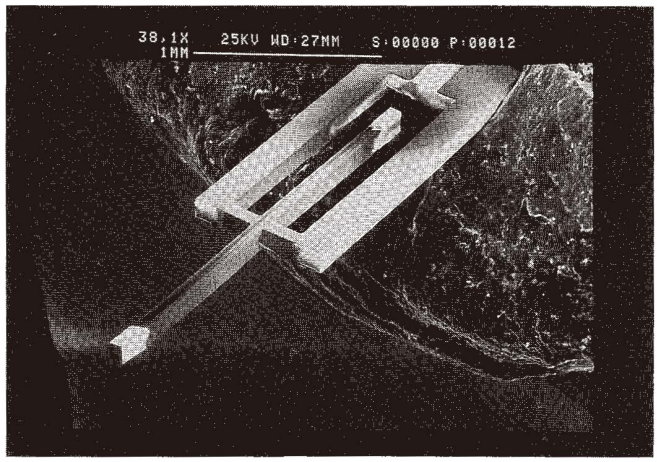

Fig. 2. SEM micrograph of an extensional-mode quartz resonator.

2. Theoretical

Hydrodynamic and electrostatic fields are the subject of the investigations discussed in this paper and are introduced in the following sections. In addition, piezoelectric and elastomechanical effects must be considered in order to perform the simulation. They describe the movement of the microstructure itself and need not be considered in this theoretical introduction.

2.1 *Electrostatics*

If an electrical voltage is applied between a polysilicon cantilever and its substrate, the nature of the force governing the movement of the cantilever will be electrostatic. The cantilever moves down to the substrate until the overall force is zero, which means that the reaction force of the cantilever must be equal to the electrostatic force acting on its surface.

Coulomb's law allows the calculation of the force $\boldsymbol{F}_{12}$ acting on charge q_1, if the vector $\boldsymbol{r}_{12}$ represents the distance and the direction from charge q_2 to charge q_1:

$$\boldsymbol{F}_{12} = \frac{1}{4\pi\varepsilon_0}\frac{q_1 q_2 \boldsymbol{r}_{12}}{|\boldsymbol{r}_{12}|^3}, \tag{1}$$

where ε_0 represents the dielectric constant. If conducting bodies are held at different potentials, forces will act on them due to charge transfer. Since the number and the location of the charges are not known in advance, the usual way of solving such problems is the introduction of the electric potential φ and its gradient, the electric field $\boldsymbol{E}$, between the bodies and the solution of the Poisson equation

$$\Delta\varphi = -\frac{1}{\varepsilon_0}\rho, \tag{2}$$

which is one of the equations governing electrostatic problems. In this equation ρ represents the charge density. If the electric field is known, the electric surface density of charges on the surface of the bodies is

$$\boldsymbol{s} = \varepsilon_0 \boldsymbol{E}, \tag{3}$$

and the area force density $\boldsymbol{f}$ can be calculated by

$$\boldsymbol{f} = \frac{1}{2}\boldsymbol{s}\boldsymbol{E}. \tag{4}$$

The overall force is obtained by integration.

2.2 *Hydrodynamics*

The hydrodynamic effects influencing oscillating microstructures can be described by the Navier-Stokes equation for incompressible fluids.

$$\frac{\partial \boldsymbol{v}}{\partial t} + \operatorname{grad}\left(\frac{v^2}{2}\right) - (\boldsymbol{v} \times \operatorname{rot}\boldsymbol{v}) = \boldsymbol{k} - \frac{1}{\rho}\operatorname{grad}(p) - \frac{\eta}{\rho}\operatorname{rotrot}\boldsymbol{v} \tag{5}$$

In this case, $\boldsymbol{v}$ designates the velocity vector, ρ the density and η the viscosity of the fluid, while the pressure is symbolized by p, and body forces such as gravitational forces by $\boldsymbol{k}$. The forces $\boldsymbol{F}$ acting on boundaries can be derived from the stress tensor σ using

$$\boldsymbol{F} = -\sigma\boldsymbol{n} = pn_i - \sigma^*_{ik}n_k = pn_i - \eta\left(\frac{\partial v_i}{\partial x_k} + \frac{\partial v_k}{\partial x_i}\right)n_k, \tag{6}$$

where $\boldsymbol{n}$ represents the vector normal to the boundary. In incompressible fluids, only transverse waves can be generated. The wavelength δ of a wave oscillating with a frequency ω can be described by

$$\delta = \sqrt{\frac{2\eta}{\omega\rho}}, \tag{7}$$

which is also the depth of penetration for these waves. The expansion of the flow is caused by the movement of a body displacing the fluid. Following the arguments of Landau and Lifschitz,[6] this flow will penetrate into the fluid to a distance corresponding to the size of the body.

3. Techniques of Modeling

3.1 *Modeling electrostatic problems*

Electrostatic problems that are to be handled numerically can be solved, for example, with the FEM program ANSYS.[7] Using the correspondence between the Poisson equation (see eq. (2)) governing the electrostatics and the Poisson equation describing the phenomena of heat conduction, the potential lines and the electric field surrounding conducting structures can be simulated. Therefore, the surrounding space is divided into nodes and thermal bricklike elements. The infinite space is represented by nodes which are far away. The nodes on the surface of the structure and for the infinite space are assigned the values of the given potential. The FEM program ANSYS generates a system of differential equations following the Poisson equation (see eq. (2)) given by the chosen nodes and elements, and attempts to solve it. The solution is a system of potential areas surrounding the structure.

ANSYS offers several tools enabling the user to interpret the results in more detail.

Most important for the present case is the calculation of the gradient of the potential lines resulting in the electrostatic field. Using eqs. (3) and (4), the surface density of the charges and the forces acting on the surface are obtained.

3.2 *Modeling hydrodynamic problems*

In this paper, hydrodynamic problems are handled by the FEM program FIDAP. The easiest way to provide the mesh for this program is to use the mesh generator of ANSYS. The advantage gained by this is that afterwards the mesh can also be used in ANSYS. This is required for the coupling of the simulation tools.

The mesh is provided in a similar way as for electrostatic simulations. The velocities of the fluid are given as boundary conditions. The FIDAP solver attempts to solve the corresponding system of differential equations, i. e., the Navier-Stokes equation (5). As a solution, the fluid velocity field is presented. Using eq. (6) the forces acting on the moving surface are obtained.

The incorporation of time dependence, when the quartz is interacting with the surrounding air, is achieved by a subroutine providing the velocity at surface nodes at certain times. These velocities can also be read from external files, i. e. ASCII files.[8]

3.3 *Movement of mesh*

The displacement of the microstructure is part of the investigation. This displacement results in deformation of the mesh used for the simulation. To modify the mesh according to the changed conditions it must be moved. The mesh movement can be calculated by replacing the edges of the thermal elements used for the electrostatic simulation with line elements. The change of elements is achieved by writing an ANSYS routine that selects each thermal element, replaces its edges by line elements and deletes the selected thermal element. Generally, it is not necessary to change the entire thermal mesh into a mesh with line elements, but only a small region around the moving structure. These line elements are treated as interconnected beams. Hence, the movement of the nodes on the surface, which is introduced as a boundary condition in the following structural analysis of the mesh of line elements, leads to movement of the nodes in the surrounding space, while the outermost nodes of this mesh-movement simulation are kept in place. This method only uses tools available in the FEM program. In this way, a mesh adapted to the movement of the microstructure is created.

By incorporating thermal expansion of each of the beams and setting a defined temperature at each beam, a mesh-optimizing routine can be created. This routine is able to adapt the positions of the nodes according to local errors occurring during the thermal or electrostatic simulation.

After the mesh-movement routine, the new calculated node positions are assigned to the mesh used for the thermal or electrostatic simulation.

3.4 *Coupling different simulation tools*

Using the results of a simulation routine to create boundary conditions for a second simulation routine is the aim of coupling different simulation tools in our case. The coupling can be done on a simple level if the nodes and the elements of the coupled meshes

are basically the same, for instance, as in the coupling between the mesh-movement routine and the thermal analysis. The coordinates of the nodes and the characteristics of the elements are stored in files, preferably ASCII coded. Results of the first simulation routine are then stored, i. e., the new nodal coordinates are stored in the corresponding file, and can be read by the second routine.

The incorporation of surface forces is slightly more complicated since the easiest way to handle them is by applying surface elements, which usually are not necessary for the simulations in the first place. During the generation of the mesh, those surface elements are created and stored in a separate file. The normal of the surface of the elements must be defined as being in the same direction in every model. The surface forces in dimensions of pressure are stored together with their corresponding surface element number so that the second program is able to read the forces acting on each surface element.

Different cases demand that different types of meshes be coupled. As an example, the structure of the mesh used for an elastomechanic simulation differs from that of the mesh applied during an electrostatic simulation. This means that the nodes defining the surface of the simulated microstructure are not the same in the two models. The FEM programs usually provide interpolation routines for such situations. The results of the first simulation, i. e., the potential lines, are interpolated on the boundary nodes of the mesh necessary for the second simulation. In some cases, especially in time-dependent problems, this interpolation step can be very time consuming and it might be more convenient to drop the use of different meshes.

4. Verification

4.1 *Electrostatic simulation of a moving structure*

In order to verify the approach comprising electrostatic simulations and movement of the mesh, a conducting sphere over a conducting infinite plane is simulated. The space around the sphere is divided into bricklike elements. "Infinite space" is represented by nodes on a hemisphere over the surface which are assigned the same potential as the plane. The distance of these "infinite" nodes from the sphere is far enough if moving these nodes has no influence on the calculated results. The nodes representing the two electrodes — "infinite space" plus the surface and the sphere — will be held at fixed potentials during the simulation. The capacitance of this system of conductors is obtained using eq. (3). Therefore, the area between neighboring nodes on the surface of the sphere is multiplied by the dielectric constant and the electric field divided by the applied voltage. The overall capacitance is obtained by summation over all surface elements of the sphere. The force acting on the sphere can be calculated in a similar manner using eq. (4).

The radius of the simulated sphere is 1 μm, while its height above the surface varies between 4 μm and 6 μm. These are nearly equal to the dimensions of the cantilever presented later. The sphere is moved from its uppermost position towards the surface using the mesh-movement routine described above.

Calculated capacitances and forces of such simulations with different meshes are shown in Fig. 3 and Fig. 4. It can be seen that the results depend strongly on the position of the nodes. In contrast, the corresponding error is rather independent of the mesh move-

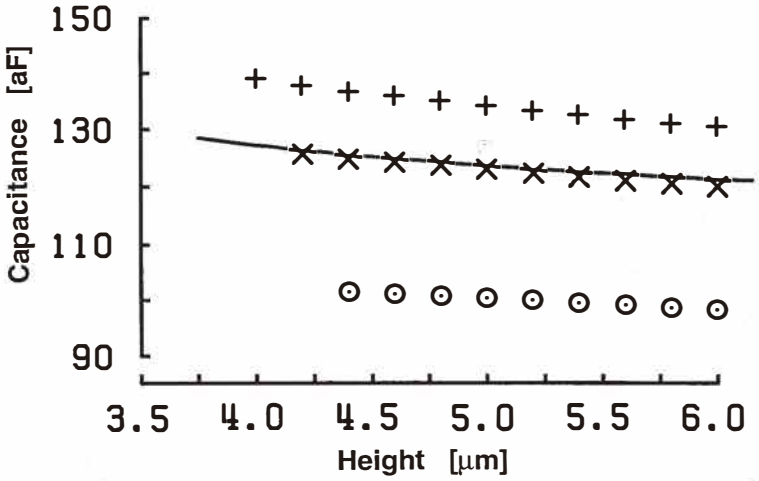

Fig. 3. Capacitance of a conducting sphere over an infinite conducting surface as a function of the height of the sphere. The parameter is the distance of the innermost nodes from the surface of the sphere. The distances are ⊙ 0.15 μm, + 0.02 μm and × 0.04 μm, while the line represents the analytical result.

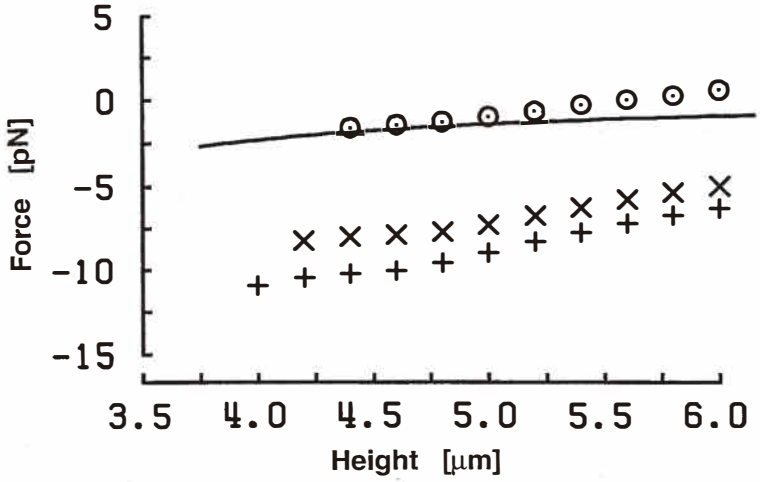

Fig. 4. Force on a conducting sphere over an infinite conducting surface as a function of the height of the sphere. The parameter is the distance of the innermost nodes from the surface of the sphere. The distances are ⊙ 0.15 μm, + 0.02 μm and × 0.04 μm, while the line represents the analytical result.

ment. This means that the qualitative behavior of the microstructure can be represented fairly well.

In order to obtain an analytical solution of the problem, the electric field is calculated using the method of conformal transformations. Snow calculated the capacitance C of a conducting sphere over an infinite conducting area.[9] If a voltage U is applied between the surface and the sphere, the energy W of this system of conductors is expressed by

$$W = \frac{1}{2} C U^2 . \tag{8}$$

The force acting on the sphere is obtained by differentiation of the energy. Figure 3 shows the capacitance of this system of conductors and Fig. 4 shows the force acting on the sphere.

4.2 *Hydrodynamic simulations*

A sphere with a radius R = 50 μm oscillating in air can be simulated with the FEM program FIDAP. Therefore, the surrounding space is represented by a cubic mesh of nodes and bricklike elements. Infinite space is described by nodes at a great distance. In this analysis, the movement of the sphere is represented by time-dependent velocities at the nodes representing the surface of the sphere.[9] The force acting on the surface is obtained using eq. (6). The overall force is calculated by integration. The problem involved in this method is the size of the mesh and the distance between the nodes since the number of nodes and elements is restricted due to the capacity of the computer. An example of such a mesh is shown in Fig. 5. The forces are obtained using eq. (6). In the following, the forces obtained by simulation with different kinds of meshes are compared with the analytical result. The force acting on this sphere oscillating with a frequency of 1 MHz is shown in Fig. 6 with respect to time.

Following the argument of Landau and Lifschitz,[6] the force acting on a sphere with a radius R oscillating sinusoidally with a velocity u and frequency ω in air can be calculated as

$$F = 6\pi\eta R\left(1 + \frac{R}{\delta}\right)u + 3\pi R^2 \sqrt{\frac{2\eta\rho}{\omega}}\left(1 + \frac{2R}{9\delta}\right)\frac{du}{dt}. \tag{9}$$

Table 1 shows the difference in the phase between simulated and analytically calculated forces acting on the surface, when the innermost nodes are defined at different distances from the surface of the sphere. The simulated and the analytically calculated forces are in phase if the innermost node is closer than 2.2 μm to the surface of the sphere. This is the penetration depth of transverse waves in air at this frequency.

The amplitude of the force depends strongly on the size of the mesh. In Table 2, the size of the outermost edge of the mesh is varied from 200 μm to 800 μm. The best simulated results can be obtained when the size of the mesh is about 400 μm which means that the distance of the outermost nodes from the surface of the sphere is about 150 μm. This is

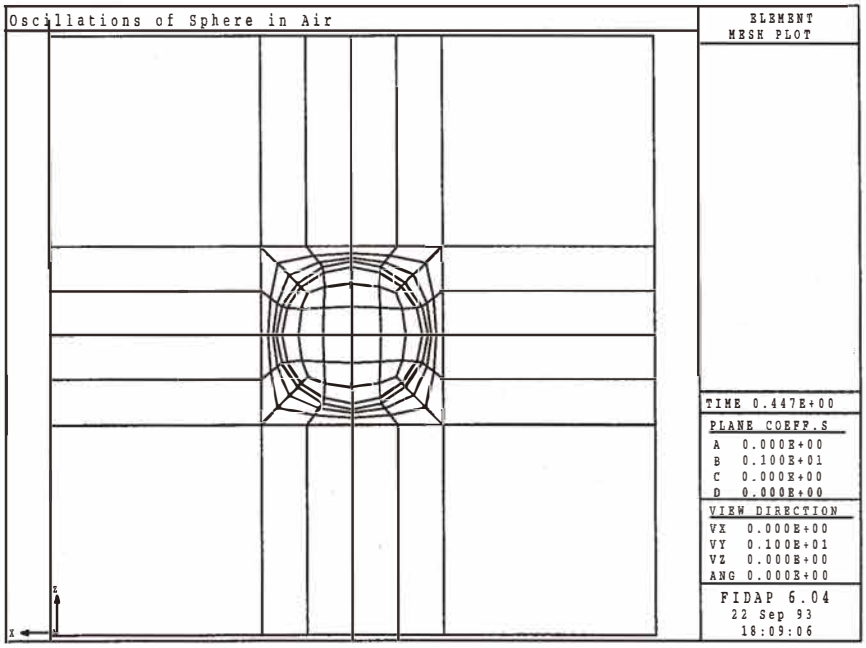

Fig. 5. Mesh used for simulation of a sphere oscillating in air.

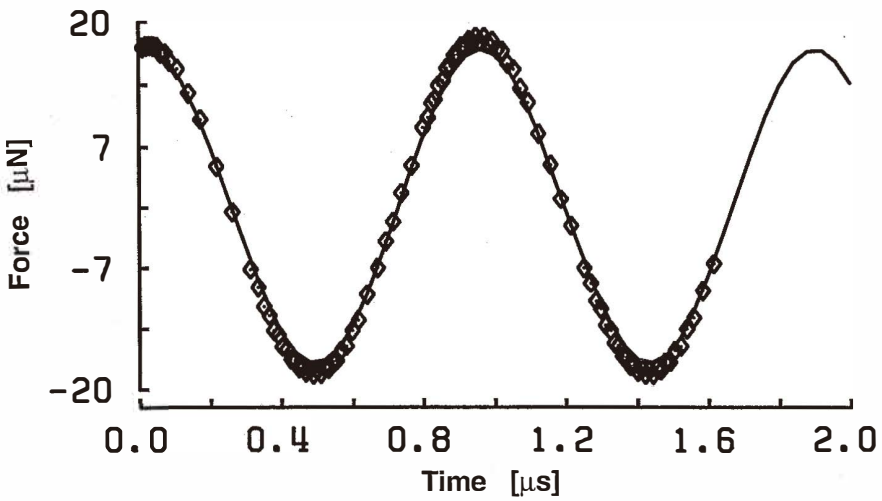

Fig. 6. Force on a sphere oscillating in air with a frequency of 1 MHz. ◊ represents the simulated results, while the analytical results are shown as a line.

Table 1
Difference of phase between the force obtained from the simulation and the analytically calculated force as a function of the distance from the innermost node to the surface of the sphere.

Distance of innermost node (μm)	2	4	6
Difference of phase (rad)	0	0.0857	0.1037

Table 2
Difference between the amplitude obtained in the simulation of the oscillating sphere and the analytically calculated amplitude of this oscillation as a function of the size of the mesh.

Length of the edge of the mesh (μm)	200	400	500	600	800
Difference of amplitude of force (μN)	–2.6	0.0	0.8	1.4	2.7

roughly the size of the sphere, hence, following the arguments of Landau and Lifschitz[6] mentioned above, the behavior can be explained. Choosing the correct size of the mesh is quite difficult. The size of the mesh can be used as a free parameter to couple the experimental results with the simulation.

It follows that this principle is applicable for microstructures oscillating in air if the mesh is chosen according to the dimensions of the moving structure. Based on this experience, the characteristics of meshes used for the following hydrodynamic simulations are chosen: the innermost nodes will be closer to the surface than the penetration depth and the size of the mesh will be approximately the same as that of the oscillating structure.

5. Simulation

5.1 *Cantilever under influence of applied forces*

The simulation of the moving cantilever requires four different meshes. The space surrounding the cantilever is divided on the basis of experience obtained from the simulation of the conducting sphere over a conducting infinite plane. This leads to the mesh for the simulation of the electrostatic field and the mesh for the mesh-movement routine. The cantilever itself is divided into structural elements simulating a material with the mechanical properties of polysilicon. As mechanical constants, a density of 2300 kgm^{-3}, Young's modulus of 170 GPa and a modulus of shear elasticity of 66 GPa were assumed.[10] Two layers of elements with Young's modulus five orders smaller form the fourth mesh. These two layers are added to the structural mesh and extend into the surrounding area in such a manner that the elastic behavior of these layers does not influence the behavior of the cantilever during simulation. These layers are used to couple the electric simulation with the structural simulation. The electric field at the surface, i. e., at provided surface elements, is obtained by the interpolation of the simulated potential of the electrostatic simulation on the outermost nodes of these two layers and resimulation of the potential lines in the mesh provided by these two layers. The resulting electric field at the surface

elements is used to calculate the forces acting on the cantilever. As mentioned above, during the structural simulation these elements are moved with the structure, but do not influence the results of the structural analysis. By interpolating this movement to the nodes on the surface of the cantilever and the nodes of the electrostatic mesh, the two introduced layers are also used for this interpolation; a mesh-displacement routine can be started as explained above. The resulting movement of the nodes is transferred to the mesh used for the electrostatic simulation.

A diagram describing the coupling of the four simulation routines is shown in Fig. 7. The applied voltage is used as input into the simulation of the electrostatic field surrounding the cantilever. The field is interpolated on the two layers and the forces acting on the cantilever are thus obtained. The forces cause a deflection of the cantilever. The motion is used as input for the subsequent mesh-displacement routine. New nodal coordinates for the electrostatic mesh are the result of the mesh-displacement routine. The program continues running in this loop until the difference in the deflection of the nodes representing the cantilever between two iterations does not exceed a preset value.

The simulation is carried out for a cantilever which is 114 μm long, 21.5 μm wide, 1 μm thick and 2 μm above the ground. The resulting deflections, for the applied voltage of 1 V, are shown in Fig. 8. Figure 9 presents a comparison of experimental and simulated results. The measured deflection is normalized by the height of the cantilever above ground. The simulated deflections of the cantilever agree within the error levels sketched in Fig. 9 with the measured deflections. As reported by Petersen,[11] the cantilever is deflected down towards the substrate if the applied voltage exceeds a threshold value. A similar effect occurs in our model with voltages exceeding 18 V. With higher voltages, the iteration routine stops as a result of the extreme deformation of the electrostatic mesh.

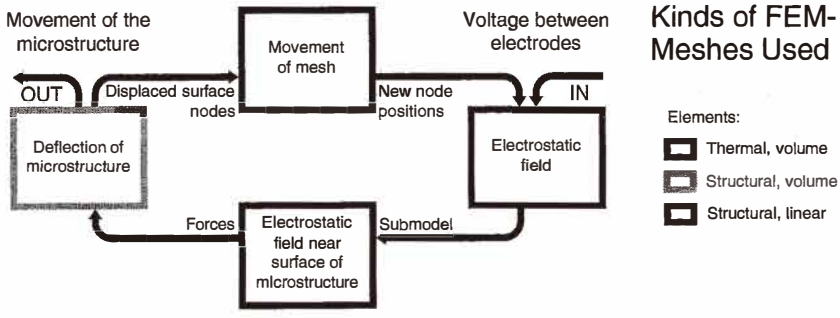

Fig. 7. Schematic data flow describing the coupling of four simulation routines in order to simulate the deflection of a microstructure under the influence of an electrostatic field.

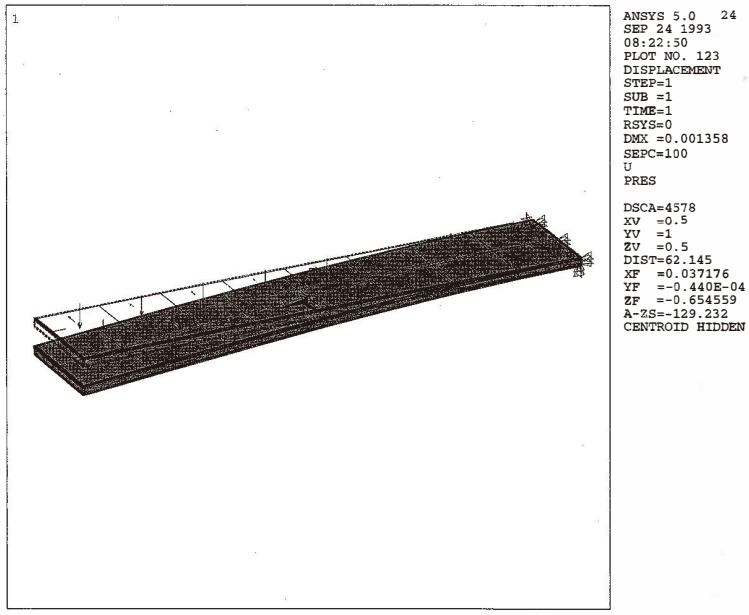

Fig. 8. Deflection of a cantilever under the influence of an electrostatic field.

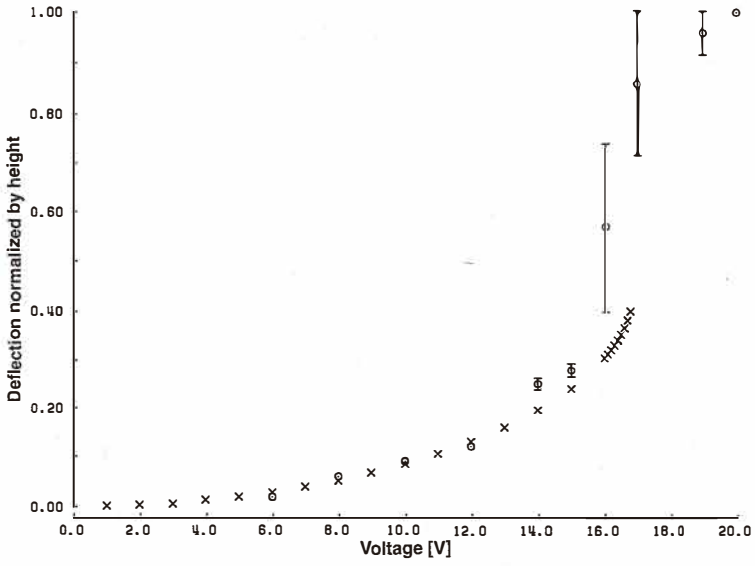

Fig. 9. Comparison of the simulated × and measured ⊙ deflection of a cantilever normalized by the height above the substrate as a function of the applied voltage.

5.2 *Tuning-fork quartz resonator oscillating in air*

A simulation of one tine of a tuning-fork resonator oscillating in air is now presented. The assumption that there is a linear gradient of the velocity of the air between the sample surface and tuning fork, made by Güthner,[3] is compared with the results of the simulation.

One tine of the resonator is simulated while it is oscillating parallel to a fixed surface. The frequency of the oscillation is 32 kHz. The velocity field is shown in Fig. 10. Figure 11 presents the velocity parallel to the velocity of the oscillator over the distance to the fixed surface. The superposition of a linear velocity gradient due to the movement of the surface of the quartz parallel to the fixed surface and a parabolic flow can clearly be seen. The parabolic flow is a result of the increasing pressure in front of the resonator and the decreasing pressure behind it.

In the future, different orientations of the tuning fork must be tested in order to verify which flow, linear or parabolic, is responsible for sensitivity and selectivity in measuring the profile of a surface while the resonator is moved over it. Also, the effects of the second tine will be investigated.

5.3 *Extensional-mode quartz resonator oscillating in air*

The first step of a simulation of this kind lies in the choice of an appropriate mesh. According to the information obtained by simulating the oscillating sphere, the size of the mesh elements should be approximately equal to the length of the oscillating resonator. In the present simulation, the quartz is 1330 μm long in the y-direction, its cross section being 80 μm $\times$ 120 μm. The mesh exhibits a cross section of 1.8 mm^2 around the moving tip of the resonator, while towards the fixed end of the resonator, the mesh is much thinner. Figure 12 shows the elements used to model the resonator, while Fig. 13 shows a view of the overall mesh. It must be emphasized that the quartz and the surrounding space are meshed in one step with the mesh generator of ANSYS. Following a piezoelectric simulation of the quartz with ANSYS, the movement of its boundary is incorporated into several single FIDAP simulations, one for each frequency of the resonator. The air flow is simulated in the same manner. The reaction forces on the surface of the quartz are calculated according to the methods presented during the description of the oscillating sphere, and incorporated in a second piezoelectric simulation as boundary conditions. The coupling of the simulation tools is shown schematically in Fig. 14. This figure also shows a possible coupling with the simulation program SPICE simulating the electrical driving circuit.

The electrical behavior of the quartz resonator simulated in vacuum is shown in Figs. 15 and 16. A frequency shift and damping effects can be seen, although the accuracy of the simulation is not yet high enough to compare quantitative results with experimental results because of the limitation on computing time.

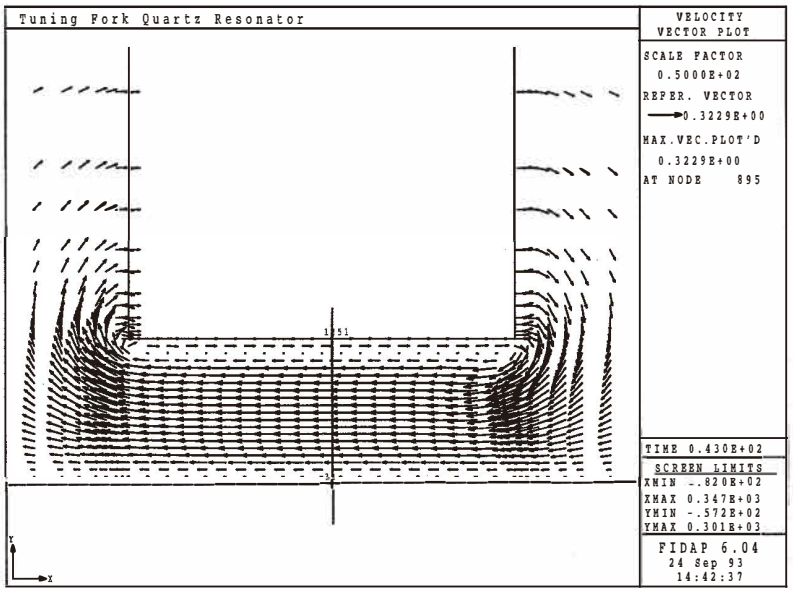

Fig. 10. Example of the velocity field of the air around the tip of one tine of a tuning-fork resonator oscillating over a fixed surface. The results were obtained by a simulation with FIDAP.

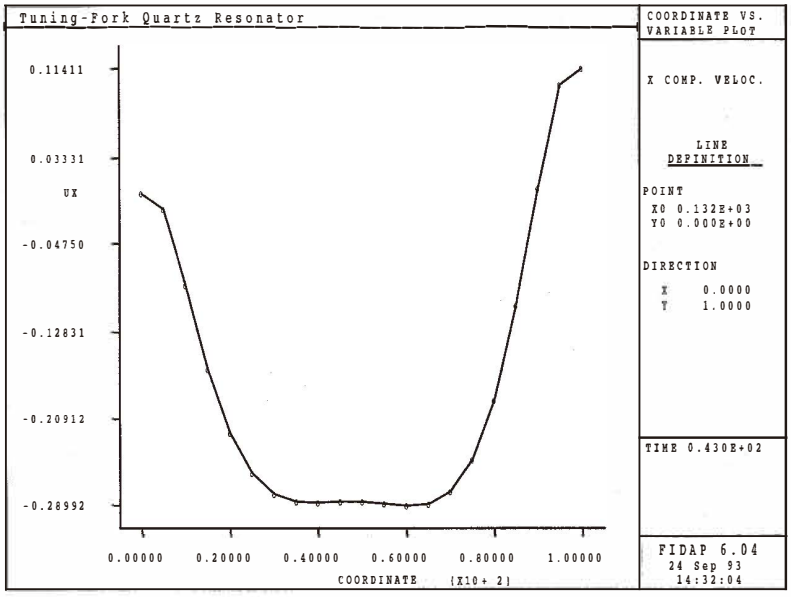

Fig. 11. Velocity of the air in the x-direction (see Fig. 10) as a function of the distance between the tine of the tuning-fork resonator and the fixed surface along the line sketched in Fig. 10. The air stream is a superposition of a linear velocity gradient and a parabolic flow.

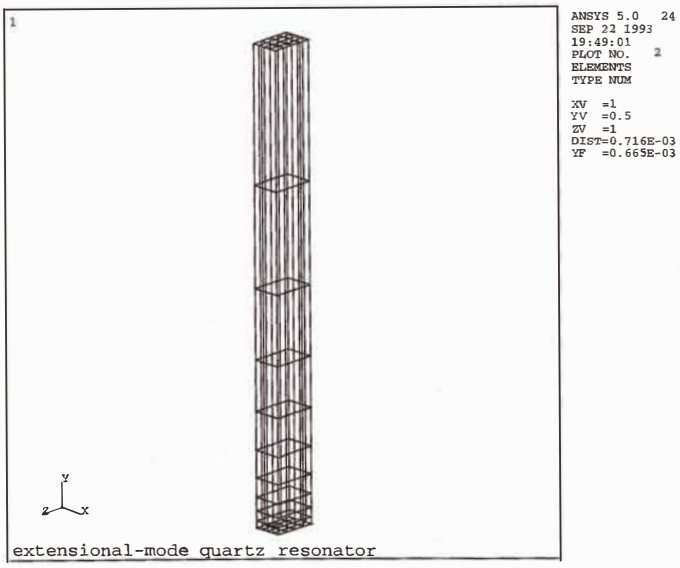

Fig. 12. Elements used to simulate the extensional-mode quartz resonator. These elements are used to transfer the calculated surface forces of the surrounding air simulated by FIDAP to the piezoelectric oscillations simulated by ANSYS. The resonator is fixed at the top, while the electrodes are on the surfaces parallel to the x-axis.

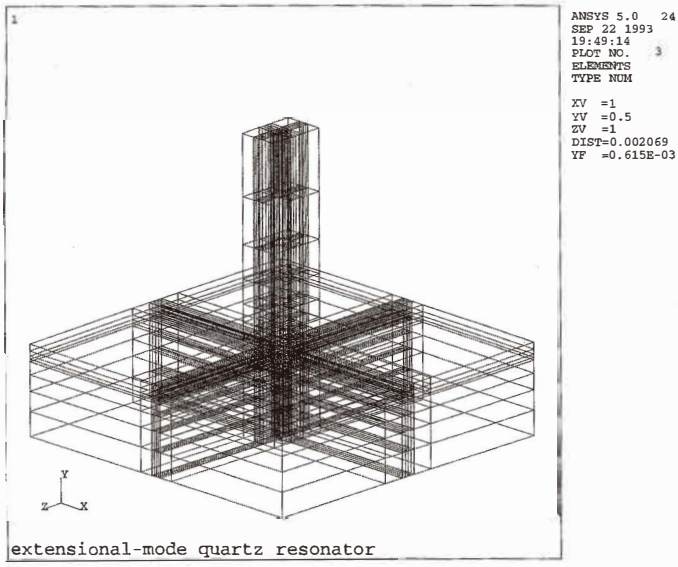

Fig. 13. Mesh to simulate the air flow around an extensional-mode resonator. The resonator is represented by the lighter elements (see Fig. 12) and is fixed at the top and moving at the bottom.

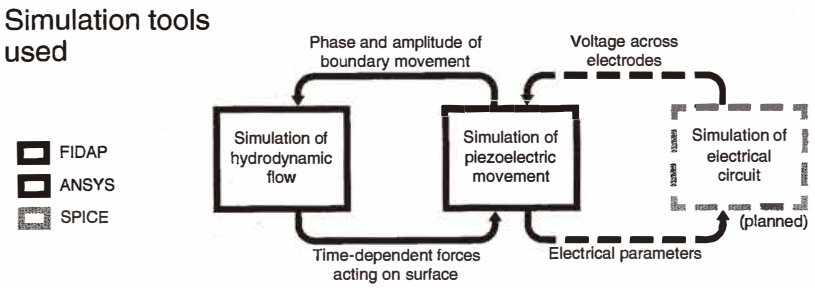

Fig. 14. Schematic data flow describing the coupling of ANSYS and FIDAP in order to simulate the influence of hydrodynamic forces on a quartz resonator oscillating in air. The future coupling with SPICE is also indicated.

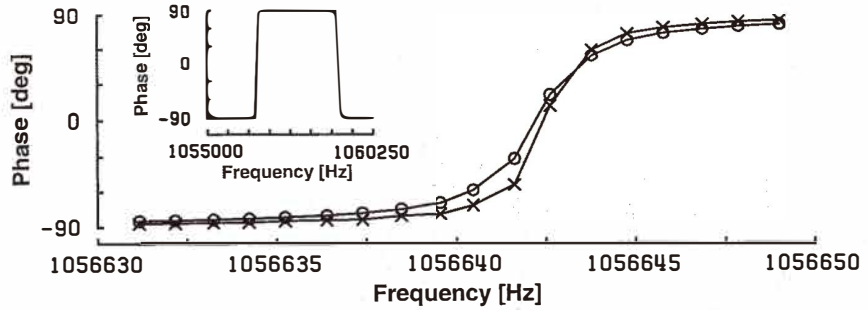

Fig. 15. Phase of the extensional-mode quartz resonator as a function of the frequency. The inset shows the results of the simulation of the resonator in vacuum. Here, the results of the simulation of the resonator in vacuum are represented by ⊙, and × represents the results of the simulation of the resonator in air. The influence of air results in a broadened resonance curve as expected.

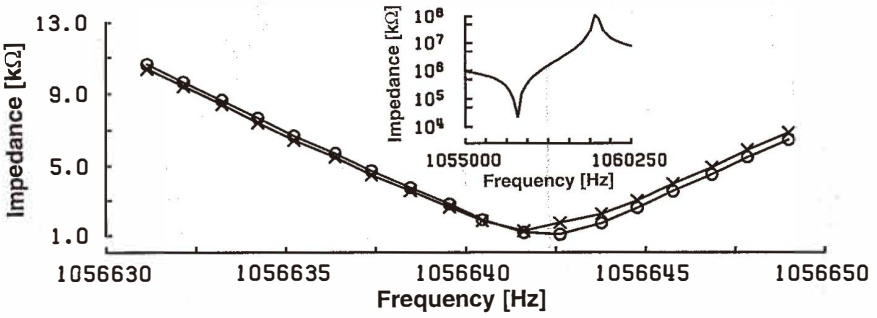

Fig. 16. Impedance of the extensional-mode quartz resonator as a function of the frequency. The inset shows the results of the simulation of the resonator in vacuum. Here, the results of the simulation of the resonator in vacuum are represented by ⊙, and × represents the results of the simulation of the resonator in air.

6. Conclusions

In this paper, it was shown that the behavior of microstructures can be simulated by coupling different commercially available simulation tools like ANSYS and FIDAP. The effects of external fields acting on movable microstructures can be incorporated into the simulations. These coupled simulation tools can be used instead of experiments. Therefore it is not necessary to develop new specific programs because commercially available FEM programs are suitable for solving different problems.

The accuracy of these simulations has been tested by comparison with analytically solvable problems and it was confirmed that the relative error of such simulations is fairly small.

The behavior of a polysilicon cantilever under the influence of an applied electrostatic field and air damping effects acting on a vibrating quartz resonator have been modeled as examples. The comparison with experimental results confirmed the accuracy of the described method. In this way the simulations have shown that these routines permit the modeling of the properties of microstructures and reveal interesting information about the interactions governing their nature. This supports the assumption that the microscopic results such as the velocity field around an oscillating quartz tip, not achievable with other methods, can be derived from such simulations. The presented method allows the use of these tools for optimization purposes. An adaptation of the simulations to quantitative behavior of the microstructures can be achieved by changing the characteristics of the mesh used.

Acknowledgments

This work was partly sponsored by the Deutsche Forschungsgemeinschaft (DFG) under project AS 44/9-1. The authors would like to thank the ANSYS and FIDAP support groups for their kind assistance, Dr. B. Studer and Dr. W. Zingg at Micro Crystal Div. of ETA, Grenchen, Switzerland for supplying the quartz resonators and Mr. J. Schaepperle and Mrs. G. Schütze for their help in preparing the manuscript.

References

1 J. G. Korvink, J. Funk and H. Baltes: Sensors and Materials **6** (1994) 235.
2 T. J. Sheerer, W. E. Nelson and L. J. Hornbeck: Seventeenth Nastran User Colloquium, NASA Conf. Publ. 3029 (1989) p. 290.
3 P. Güthner: Untersuchung der lokalen piezoelektrischen Eigenschaften dünner ferroelektrischer Polymerfilme (Konstanzer Dissertationen 357, Hartung-Gorre Verlag, Konstanz, Germany, 1992).
4 M. Weinmann and F. Aßmus: VDI-Berichte 939 (VDI-Verlag, Düsseldorf, 1992) p. 453.
5 M. Weinmann, W. Engelhardt, R. Radius and F. Aßmus: Sensors and Actuators **A 37-38** (1993) 715.
6 L. D. Landau and E. M. Lifschitz: Lehrbuch der theoretischen Physik Bd. 6. (Akademie-Verlag Berlin, Germany, 1991, 5th ed.).
7 ANSYS User's Manual, Swanson Analysis Systems, Houston, PA, U.S.A., Revision 5.0, 1992.

8 Fidap User's Manual, Fluid Dynamics International, Evanston, Illinois, U.S.A. Revision 6.0, 1991.
9 Ch. Snow: Formulas for Computing Capacitance and Inductance, NBS Circular No. 544, National Bureau of Standards, United States Department of Commerce, 1954.
10 M. Fischer, H. Graef and W. von Münch: Sensors and Actuators **A 44** (1994) 83.
11 K. E. Petersen: IEEE Trans. Electron. Devices, ED-25 (1978) 1241.